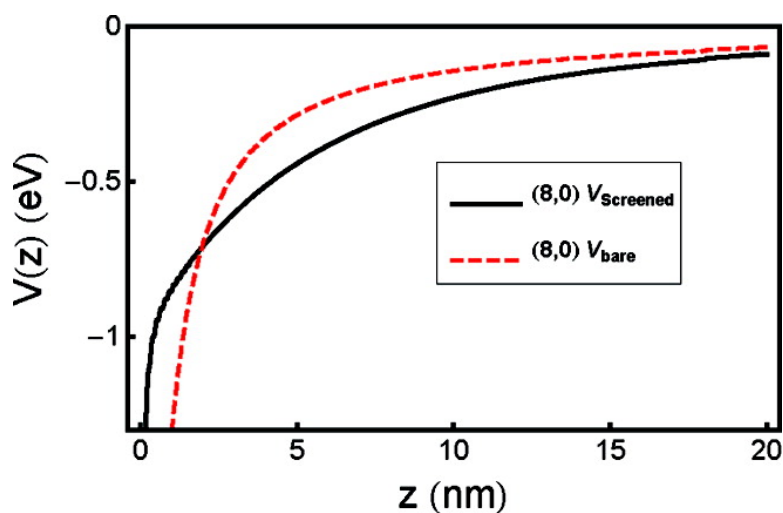


Electron-Hole Interaction in Carbon Nanotubes: Novel Screening and Exciton Excitation Spectra

Jack Deslippe, Mario Dipoppa, David Prendergast, Marcus
V. O. Moutinho, Rodrigo B. Capaz, and Steven G. Louie

Nano Lett., **2009**, 9 (4), 1330-1334 • DOI: 10.1021/nl802957t • Publication Date (Web): 09 March 2009

Downloaded from <http://pubs.acs.org> on May 14, 2009



More About This Article

Additional resources and features associated with this article are available within the HTML version:

- Supporting Information
- Access to high resolution figures
- Links to articles and content related to this article
- Copyright permission to reproduce figures and/or text from this article

[View the Full Text HTML](#)



ACS Publications
High quality. High impact.

Nano Letters is published by the American Chemical Society, 1155 Sixteenth Street N.W., Washington, DC 20036

Electron–Hole Interaction in Carbon Nanotubes: Novel Screening and Exciton Excitation Spectra

Jack Deslippe,^{†,‡} Mario Dipoppa,^{†,‡,§} David Prendergast,^{†,||}
Marcus V. O. Moutinho,[⊥] Rodrigo B. Capaz,[⊥] and Steven G. Louie^{*,†,‡}

Department of Physics, University of California at Berkeley, Berkeley, California 94720, Materials Sciences Division, Lawrence Berkeley National Laboratory, Berkeley, California 94720, Ecole Normale Supérieure de Lyon, 69364 Lyon, France, Molecular Foundry, Materials Sciences Division, Lawrence Berkeley National Laboratory, Berkeley, California 94720, and Instituto de Física, Universidade Federal do Rio de Janeiro, Caixa Postal 68528, Rio de Janeiro, RJ 21941-972, Brazil

Received September 29, 2008; Revised Manuscript Received January 13, 2009

ABSTRACT

The optical response of single-walled carbon nanotubes is dominated by exciton states with unusually large binding energies. We show that screening in semiconducting tubes enhances rather than reduces the electron–hole interaction for separations larger than the tube diameter. This “antiscreening” region deepens the relative energy level of the higher exciton states yielding unconventional excitation spectra. The effect explains the discrepancy in the current experimentally extrapolated exciton binding energies (deduced using conventional model spectra) and those obtained from *ab initio* calculations on isolated tubes.

In single-walled carbon nanotubes (SWCNT), due to quasi-one-dimensionality, the interaction between an optically excited electron and hole is expected to be significantly stronger than that in three-dimensional bulk systems.^{1,2} This leads to the prediction of strongly bound exciton states (electron–hole correlated pair states) for both semiconducting and metallic SWCNTs, with binding energies as large as 1 eV for the lowest optically allowed states for semiconducting tubes² and 50–100 meV for metallic tubes.^{2,3} Subsequent experiments on the one- and two-photon optical transitions in semiconducting SWCNTs^{4–7} have confirmed the strong excitonic picture of the optically excited states, and recent absorption measurements⁸ also provided evidence of excitons in metallic SWCNTs. However, in obtaining the exciton binding energies in semiconducting tubes from the two-photon experiments, which are performed on tubes in a dielectric medium, theoretical input is required because the experiments measure directly only the difference between the energy of the lowest (E_{1A_2}) and the second lowest (E_{2A_1}) optically active exciton states.²¹ The binding energy of the

lowest exciton may be evaluated directly from *ab initio* calculations employing the GW–Bethe–Salpeter equation (GW-BSE) technique^{2,9,10} as $E_{1A_2}^{\text{bind}} = E_{\text{cont}} - E_{1A_2}$ where E_{cont} is the onset energy of the electron–hole continuum. However, experimental estimates of $E_{1A_2}^{\text{bind}}$ in the literature, which have been extrapolated from measurements of $(E_{2A_1} - E_{1A_2})$ employing a particular 1D model potential for the electron–hole interaction with a constant dielectric function playing the role of the environment^{4,5} resulting in an empirical rule of $E_{1A_2}^{\text{bind}} \approx 1.4(E_{2A_1} - E_{1A_2})$, are significantly lower than the *ab initio* results. In addition, more recent measurements on isolated tubes^{6,7} have observed excitonic spectral peaks at energies that are significantly higher above the E_{1A_2} value than the empirically assumed binding energies.

In this work, we show that the exciton binding energy from model calculations is sensitive to the form and accuracy of the model potential and that this is the source of the discrepancy between model derived experimental and *ab initio* values. The absorption spectrum changes drastically depending on whether a model with constant dielectric screening or spatially dependent dielectric screening is used, which explains the discrepancy in the literature regarding both the $1A_2$ exciton binding energy and the energy spacing of higher excited states. To this end, we formulate a new physically grounded model for the effective 1D electron–hole interaction of both semiconducting and metallic isolated

* Corresponding author, sglouie@berkeley.edu.

[†] Department of Physics, University of California at Berkeley.

[‡] Materials Sciences Division, Lawrence Berkeley National Laboratory.

[§] Ecole Normale Supérieure de Lyon.

^{||} Molecular Foundry, Materials Sciences Division, Lawrence Berkeley National Laboratory.

[⊥] Instituto de Física, Universidade Federal do Rio de Janeiro.

Table 1. Comparison of Experimental and Theoretical Values for the Exciton Excitation Energy Difference, $E_{2A_1} - E_{1A_2}$, and the Lowest Exciton Binding Energy $E_{1A_2}^{\text{bind}}$ (in eV)

	$E_{2A_1} - E_{1A_2}$		$E_{1A_2}^{\text{bind}}$		ab initio (extrap)
	expt (measured)	present work	expt (extrap)	present work	
(6,4)	0.33 ^b	0.41	0.42 ^b	0.98	0.91 ^c
(6,5)	0.31 ^a , 0.28 ^b	0.38	0.43 ^a , 0.37 ^b	0.85	0.81 ^c
(7,5)	0.28 ^a , 0.23 ^b	0.34	0.39 ^a , 0.31 ^b	0.77	0.77 ^c
(7,6)	0.20 ^a	0.31	0.35 ^a	0.70	0.70 ^c
(8,3)	0.30 ^a , 0.29 ^b	0.37	0.42 ^a , 0.38 ^b	0.84	0.84 ^c
(8,6)	0.25 ^a	0.28	0.35 ^a	0.64	0.66 ^c
(8,7)	0.20 ^a	0.26	0.29 ^a	0.60	0.61 ^c
(9,1)	0.32 ^b	0.38	0.42 ^b	0.88	0.87 ^c
(9,4)	0.24 ^a , 0.27 ^b	0.30	0.34 ^a , 0.38 ^b	0.69	0.71 ^c
(9,5)	0.23 ^a	0.28	0.33 ^a	0.62	0.62 ^c
(9,7)	0.22 ^a	0.24	0.30 ^a	0.55	0.58 ^c
(10,2)	0.24 ^a	0.31	0.34 ^a	0.73	0.75 ^c
(11,3)	0.22 ^a	0.27	0.31 ^a	0.62	0.65 ^c
(11,6)	0.19 ^a	0.21	0.27 ^a	0.51	0.55 ^c
(12,4)	0.20 ^a	0.21	0.27 ^a	0.53	0.58 ^c

^a From refs 4 and 11. ^b From ref 5. ^c From ref 12.

SWCNTs, including the important effects of a spatially dependent dielectric function, that is in agreement both with measurement and ab initio calculations. We show that because of the unique nature of screening in one-dimensional systems, the electron–hole interaction is strengthened (as compared to the bare interaction) rather than weakened at electron–hole separation distances typical in higher excitonic states such as the $2A_1$, $3A_2$, $4A_1$, etc., which causes these states to have a binding energy that is a larger fraction of the lowest state $1A_2$ binding energy than in previous models considered.^{4,11}

The two-photon optical transition experiments of Wang et al.⁴ directly measured the energy difference between the excitation energies of the lowest even envelope function exciton state, E_{1A_2} , and of the first odd envelope function exciton state, E_{2A_1} , within a given interband transition complex. The binding energy of the lowest energy state, $E_{1A_2}^{\text{bind}}$, was then estimated by fitting the measured value of $(E_{2A_1} - E_{1A_2})$ to the difference between the two lowest quantum states of the following 1D hydrogenic-like potential by varying the parameter ϵ

$$V_h(z) = \frac{-e^2}{(|z| + z_0)\epsilon} \quad (1)$$

where $z_0 = 0.3d$ is a parameter approximating the diameter (d) dependence of the interaction. Using this potential form, a binding energy of approximately $E_{1A_2}^{\text{bind}} \approx 1.4(E_{2A_1} - E_{1A_2})$ was found. The value of the binding energy for the tubes studied ((7,5), (6,5), and (8,3)) were significantly lower than those predicted by extrapolations based on the ab initio calculations of Spataru et al.^{2,12} (see Table 1). In the ab initio calculation on the (8,0), (10,0), and (11,0) nanotubes, for example, the binding energy, $E_{1A_2}^{\text{bind}}$, was approximately two to three times that of the calculated $E_{2A_1} - E_{1A_2}$ values, revealing the inadequacy of the model interaction given in eq 1 and casting doubt on the accuracy of empirically extrapolated binding energies based on it for isolated SWCNTs.

The most unphysical approximation in using eq 1 to model the effective electron–hole interaction in isolated SWCNTs is the use of a constant dielectric screening, represented by the parameter ϵ . Another approximation is the particular form of the diameter dependence in eq 1. We seek a more accurate description of the effective 1D electron–hole interaction in SWCNTs, which in principle could be extended to other 1D structures. From the Bethe–Salpeter equation,¹⁰ one can show that, within the usual effective mass approximation, the exciton binding energy E_{ex} and envelope function $F(z)$, for a given state, satisfy

$$\left[-\frac{\hbar^2}{2m^*} \frac{\partial^2}{\partial z^2} - V_{\text{dir}}(z) + J\delta(z) \right] F(z) = E_{\text{ex}} F(z) \quad (2)$$

where J is the exchange integral between the valence and conduction states at the band minima and

$$V_{\text{dir}}(z') = \int dx' dy' d\vec{r}_2 W(\vec{r}' + \vec{r}_2, \vec{r}_2) \rho_c(\vec{r}' + \vec{r}_2) \rho_v(\vec{r}_2) \quad (3)$$

is the direct interaction, where, $\rho_c = |\psi_c(\vec{r})|^2$ and $\rho_v = |\psi_v(\vec{r})|^2$, and W is the screened Coulomb interaction. The interaction, V_{dir} , corresponds to a weighted average of W over the electron–hole relative coordinates perpendicular to the tube axis (x', y') and the position of the center of mass throughout one unit cell.

To obtain a model that is useful for SWCNTs of arbitrary chirality and diameter, it is necessary to find analytic expressions for eq 2 and eq 3. For simplicity, we first neglect the exchange term, $JF(0)$, which is responsible for the singlet/triplet splitting of the exciton states. This is justified by noting that the singlet/triplet splitting from ab initio study is approximately 10–50 meV¹³ for the (8,0), (10,0), and (11,0) SWCNTs, whereas the exciton binding energies are on the order of 1 eV. Second, we approximate that $\rho_c(s, \theta, z) = \rho_v(s, \theta, z) = (1/\pi d L) \delta(s - (d/2))$, where s is the radial coordinate perpendicular to the tube axis, L is the length of a unit cell, and d is the tube diameter; i.e., the charge exists uniformly on the surface of a cylinder of diameter equal to that of the SWCNT studied. The unscreened 1D electron–hole interaction under this approximation is that of two rings (in atomic units)

$$V_{\text{bare}}(z) = \frac{\frac{2}{\pi} K \left(-\frac{d^2}{z^2} \right)}{|z|} \quad (4)$$

where $K(z^2) = \int_0^{(\pi/2)} d\theta / (1 - z^2 \sin^2(\theta))^{1/2}$ is the complete elliptic integral of the first kind. Or in Fourier space

$$V_{\text{bare}}(q) = 2I_0 \left(q \frac{d}{2} \right) K_0 \left(q \frac{d}{2} \right) \quad (5)$$

where I_0 and K_0 are the zeroth-order modified Bessel functions of the first and second kind. This expression for the bare interaction has been used to model the 1D

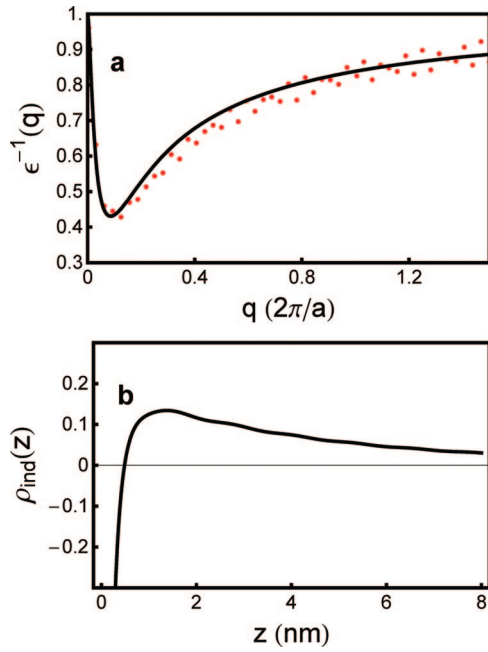


Figure 1. Dielectric screening in SWCNTs. (a) Comparison between the averaged ab initio inverse dielectric function, $\epsilon^{-1}(q)$ (data points) and the 1D ring Penn model (solid line) of the (8,0) SWCNT. The parameters C_1 and C_2 in the text were fit to give the best agreement. (b) The induced charge distribution around an added positive ring charge (at $z = 0$) plotted down the tube axis. The total induced charge integrates to zero.

electron–hole interaction in the past, but without ab initio input for the polarizability.^{8,14} We can express an effective one-dimensional dielectric function as $\epsilon(q) = 1 - \chi(q)V_{\text{bare}}(q)$ and the total screened potential from a single ring charge is then

$$V(q) = \frac{V_{\text{bare}}(q)}{1 - \chi(q)V_{\text{bare}}(q)} \quad (6)$$

For semiconducting tubes with band gap E_g and diameter d , we obtain the form of $\chi(q)$ by a 1D Penn model,¹⁵ enforcing that the exciton binding energies go to zero as $1/d$ for large d , as

$$\chi(q) \approx -\frac{C_2' d}{E_g} \frac{\alpha q^2}{1 + \alpha q^2} \approx -C_2 d^2 \frac{C_1 q^2}{1 + C_1 q^2} \quad (7)$$

where, $\alpha = C_1'/E_g^2 d^2 \approx C_1$ is a diameter-independent quantity, since the band gap of semiconducting tubes scales approximately as $1/d$. (Atomic units are used throughout.) Equations 2 and 5–7 yield an effective electron–hole interaction model for semiconducting tubes which is diameter and chirality dependent through the effective mass and the explicit diameter dependence in χ and V_{bare} .

A plot comparing $\epsilon(q) = 1 - \chi(q)V_{\text{bare}}(q)$ using eq 5 and eq 7 with the full ab initio dielectric function for the (8,0) tube is shown in Figure 1a, after fitting the two constants C_1 and C_2 to achieve the best agreement. The dielectric function has interesting characteristics that are not found in 3D

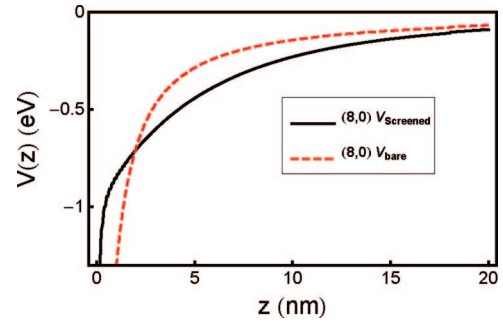


Figure 2. 1D electron–hole interaction potential. Comparison of the screened interaction for the (8,0) zigzag tube with the bare interaction, eq 5. The notable feature in this plot is the region in which the screened interaction actually drops below the bare interaction. This is a region of antiscreening that accounts for the relatively large binding energies of exciton states.

semiconductors. As was pointed out by Leonard et al.,¹⁶ the dielectric function goes to unity at both large and small q . This implies that, in 1D semiconducting systems, there is no screening at both short and large separation. In bulk semiconductors, $\epsilon(q = 0)$ is a nontrivial constant corresponding to the fact that, when viewed from large distances, there is a finite induced charge around an added external charge that screens the added charge. In SWCNTs and other reduced dimensional systems, the induced charge around an external charged particle actually integrates to zero. Using eq 6 for the total potential of an added electron in the form of a ring of charge, the induced charge, $\rho_{\text{ind}}(q) = \chi(q)V(q)$, is plotted for the (8,0) tube in real space in Figure 1b. The presence of both positive and negative induced charge density near the added charge integrating to zero is evident. This leads to the novel effect that for electron–hole separation greater than the tube diameter the electron–hole interaction is enhanced (see Figure 2).

The real space dependence of our 1D effective electron–hole interaction, eq 6, is shown in Figure 2 for the (8,0) semiconducting SWCNT. The interaction drops below $V_{\text{bare}}(z)$ in the region where screening charges of the same sign as the added charge are induced (the antiscreening region). This antiscreening behavior was seen by van den Brink and Sawatzky for molecular nanostructures^{17,18} using a simple dipole interaction model. We now show that it comes out explicitly from the first principles GW/BSE calculations and causes the higher states in the series (2A₁, 3A₂, 4A₁,...) to have binding energies that are a relatively higher fraction of the 1A₂ binding energy than is the case in a hydrogenic like electron–hole model. This is the physical origin of the failure of eq 1 in describing the excitonic spectrum of isolated SWCNTs.

We obtain the parameters C_1 and C_2 in our model by minimizing the energy difference between the solutions to eq 2 and those of the series of excitons derived from the first (E_{11}) and second (E_{22}) optically allowed interband transitions of the ab initio calculations on the (8,0), (10,0), and (11,0) tubes. For the solution of eq 2, the effective masses were taken from an interpolation formula by Jorio et al.¹⁹ The optimal values are $C_1 = 424$ and $C_2 = 0.015$, in

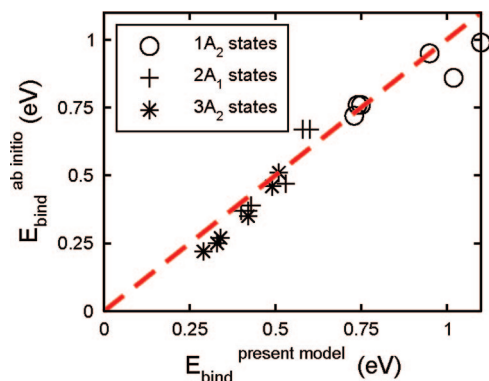


Figure 3. Comparison between ab initio and model binding energies of the $1A_2$, $2A_1$, and $3A_2$ states associated with the E_{11} and E_{22} interband transitions for the (8,0), (10,0), and (11,0) SWCNTs.

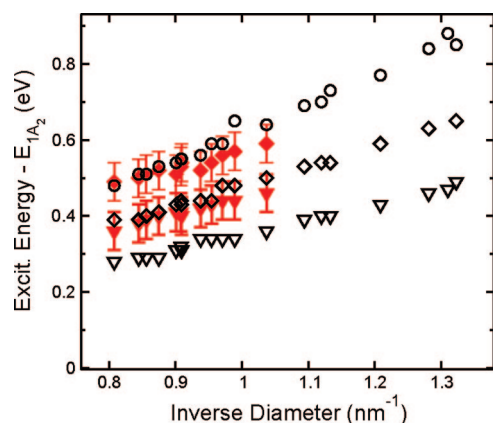


Figure 4. Comparison of the observed spectral peak positions for different diameter semiconducting tubes in the work of Lefebvre et al.⁶ to the $3A_2$ and $5A_2$ excitonic state energies in the E_{11} bound exciton series. The black circles represent the calculated continuum level in the present model while the black diamonds and triangles represent the $5A_2$ and $3A_2$ states, respectively. The red diamonds and triangles are the $L1^*$ and $L1$ features in the work by Lefebvre et al.⁶

atomic units. Figure 3 compares the binding energies from the ab initio calculation and the present model.

Table 1 shows the predicted binding energies of the present model for the tubes measured by Wang et al.⁴ and Maultzsch et al.⁵ Our model results agree to within 0.1 eV with the measured $E_{2A_1} - E_{1A_2}$ values, suggesting the dielectric environment and the antiscreening effect does not greatly change this value because the electron–hole amplitude is concentrated near the origin of Figure 2 for these states. However, the present model disagrees quite dramatically with the binding energies reported in those papers obtained by extrapolation using the relation $E_{1A_2}^{\text{bind}} \approx 1.4(E_{2A_1} - E_{1A_2})$. Owing to the spatial-dependent dielectric function (i.e., the antiscreening effect), we find that $E_{1A_2}^{\text{bind}} \approx 2.3(E_{2A_1} - E_{1A_2})$ for these tubes, showing that eq 1 underestimates the exciton binding energy of isolated SWCNTs. Shown in Figure 4 are the excitation features for tubes studied in the work of Lefebvre et al.⁶ The observed features (labeled $L1$ and $L1^*$ in ref 6) above the E_{1A_2} energy in the experimental spectra lie in the energy range of the bright $3A_2$, $5A_2$ and continuum exciton states of the E_{11} transition in the current model

Table 2. Comparison between Binding Energies for the Lowest Bound Exciton in Metallic Tubes between the Present Model, ab Initio Calculations³ and Experiment⁸ (in meV)

	present work	ab initio	experiment
(5,5) E_{11}	59	64	
(10,10) E_{11}	51	50	
(21,21) E_{22}	40		50

suggesting an assignment of these features to a higher exciton state. Also shown in Table 1 is a comparison of the current model $1A_2$ binding energies to those extrapolated from ab initio.¹² Although this extrapolation in the previous work was done using a constant dielectric function, the constant was fit in order that the $1A_2$ binding energies match those calculated from ab initio. The higher states in the current model spectra are significantly more spread out in energy than in the previous work where the $2A_1$ excitation energy is already very near the continuum energy.

For the metallic SWCNTs, we may approximate the dielectric function within a free electron Thomas–Fermi approximation. In this case, $\chi_m(q) = -D(E_F)$, where $D(E_F)$ is the density of states per unit length at the Fermi energy, E_F . To take into account the additional screening of the higher subbands, we add a tube-independent constant, $\epsilon_{\text{IB}} = 2$, to the metallic dielectric function. Because the density of states does not vary greatly with tube diameter, the number of screening electrons is approximately constant with tube diameter. Small diameter tubes, therefore, have a larger dielectric function (and consequently more screening) due to the diameter dependence of the bare Coulomb potential between charged rings.

Table 2 shows a comparison of the binding energies obtained in the present model to those from ab initio³ and experiment⁸ for the (5,5), (10,10), and (21,21) metallic SWCNTs. Again, the agreement is good. Because of the enhanced screening in smaller diameter metallic tubes, the binding energies of the excitons are relatively constant as a function of diameter compared to the scaling behavior of semiconducting tubes. Other experiments involving photocurrent-spectroscopy have also predicted binding energies of approximately 50 meV in metallic SWCNTs.²²

In summary, our analysis shows that the use of an electron–hole interaction model with a spatially constant dielectric function to estimate the $1A_2$ exciton binding energy in isolated SWCNTs leads to a large underestimation of the binding energy. Such a model may be suitable for nanotubes suspended in solution; however, the effect of a dielectric background medium on the exciton binding energies of tubes suspended in solution or in a polymer matrix remains a difficult and underexplored issue to be examined both theoretically and experimentally. We demonstrate that the exciton binding energies of isolated SWCNTs can be accurately determined through the application of an effective electron–hole interaction with spatial-dependent dielectric screening. An important “antiscreening” effect on the binding energy of the exciton states is discovered for the semiconducting tubes. The single-photon photoluminescence experiments on isolated tubes by Lefebvre et al.⁶ agree well with the current model, which provides a bridge connecting the

ab initio calculations with the experimental spectroscopic structure of isolated tubes.

Acknowledgment. This work was supported by National Science Foundation Grant No. DMR07-05941 and by the Director, Office of Science, Office of Basic Energy Sciences, Division of Materials Sciences and Engineering Division, U.S. Department of Energy under Contract No. DE-AC02-05CH11231. Computational resources have been provided by NSF at the San Diego Supercomputing Center (SDSC) and DOE at the National Energy Research Scientific Computing Center (NERSC). M.D. acknowledges funding from Masters Program International Fellowship at Ecole Normale Supérieure de Lyon, France. R.B.C. and M.V.O.M. acknowledge financial support from Brazilian agencies CAPES, CNPq, FAPERJ, Instituto de Nanotecnologia—MCT, and Rede Nacional de Pesquisa em Nanotubos de Carbono. J.D. acknowledges funding from the DOE Computational Science Graduate Fellowship (CSGF) under Grant Number DE-FG02-97ER25308. We thank S. Ismail-Beigi for helpful discussions.

References

- (1) Ando, T. *J. Phys. Soc. Jpn.* **1997**, 66 no 4, 1066.
- (2) Spataru, C. D.; Ismail-Beigi, S.; Benedict, L. X.; Louie, S. G. *Phys. Rev. Lett.* **2004**, 92, 077402.
- (3) Deslippe, J.; Spataru, C. D.; Prendergast, D.; Louie, S. G. *Nano Lett.* **2007**, 7 no 6, 1626.
- (4) Wang, F.; Dukovic, G.; Brus, L. E.; Heinz, T. F. *Science* **2005**, 308 no 5723, 838.
- (5) Maultzsch, J.; Pomraenke, R.; Reich, S.; Chang, E.; Prezzi, D.; Ruini, A.; Molinari, E.; Strano, M. S.; Thomsen, C.; Lienau, C. *Phys. Rev. B* **2005**, 72, 241402.
- (6) Lefebvre, J.; Finnie, P. *Phys. Rev. Lett.* **2007**, 98, 167406.
- (7) Lefebvre, J.; Finnie, P. *Nano Lett.* **2008**, 8 no 7, 1890.
- (8) Wang, F.; Cho, D.; Kessler, B.; Deslippe, J.; Schuck, P. J.; Louie, S. G.; Zettl, A.; Heinz, T. F.; Shen, Y. R. *Phys. Rev. Lett.* **2007**, 99, 227401.
- (9) Hybertsen, M. S.; Louie, S. G. *Phys. Rev. B* **1986**, 34, 5390.
- (10) Rohlfing, M.; Louie, S. G. *Phys. Rev. B* **2000**, 62, 4927.
- (11) Dukovic, G.; Wang, F.; Song, D.; Sfeir, M. Y.; Heinz, T. F.; Brus, L. E. *Nano Lett.* **2005**, 5 no 11, 2314.
- (12) Capaz, R. B.; Spataru, C. D.; Ismail-Beigi, S.; Louie, S. G. *Phys. Rev. B* **2006**, 74, 121401.
- (13) Spataru, C. D.; Ismail-Beigi, S.; Capaz, R. B.; Louie, S. G. *Phys. Rev. Lett.* **2005**, 95, 247402.
- (14) Bulashevich, K. A.; Suris, R. A.; Rotkin, S. V. *Int. J. Nanosci.* **2003**, 2 issue 6, 561.
- (15) Penn, D. R. *Phys. Rev.* **1962**, 128 no 5, 2093.
- (16) Leonard, F.; Tersoff, J. *Appl. Phys. Lett.* **2002**, 81 no 25, 4835.
- (17) van den Brink, J.; Sawatzky, G. A. *Europhys. J.* **2000**, 50 issue 4, 447.
- (18) van den Brink, J.; Sawatzky, G. A. *Electronic Properties of Novel Materials: Progress in Molecular Nanostructures*; AIP Conference Proceedings 442; American Institute of Physics: Woodbury, NY, 1998; p 152.
- (19) Jorio, A.; Fantini, C.; Pimenta, M. A.; Capaz, R. B.; Samsonidze, G. G.; Dresselhaus, G.; Dresselhaus, J. J. M. S.; Kobayashi, N.; Grneis, A.; Saito, R. *Phys. Rev. B* **2005**, 71, 075401.
- (20) Barros, E. B.; Jorio, A.; Samsonidze, G. G.; Capaz, R. B.; Filho, A. G. S.; Filho, J. M.; Dresselhaus, G.; Dresselhaus, M. S. *Phys. Rep.* **2006**, 431, 261.
- (21) We label the exciton states by $n\Gamma$, where $n-1$ is the number of nodes in the envelope function and Γ labels its irreducible representation in the “group of the wave vector” formalism.²⁰ Therefore, $1A_2$ refers to the lowest one-photon-bright exciton with a zero-node envelope function (sometimes also labeled $1u$, $1s$, or $0A_0^-$) and $2A_1$ refers to the two-photon-bright exciton with a one-node envelope function (sometimes also labeled $2g$, $2p$, or $0A_0^+$ in the literature). This notation is for chiral tubes. For zigzag tubes, the proper notation would be $1A_{2u}$ and $2A_{1g}$, but we omit this difference for simplicity. Unless otherwise noted, we are always referring to excitons associated with the lowest optically allowed, E_{11} , interband transition.
- (22) Mohite, A.; Lin, J.-T.; Sumanasekera, G.; Alphenaar, B. W. *Nano Lett.* **2006**, 6 (7), 1369.

NL802957T